AIAA JOURNAL
Vol. 51, No. 2, February 2013

Dynamic Elasticity Solution for the Transient Blast Response of Sandwich Beams/Wide Plates

G. A. Kardomateas,* Y. Frostig,† and C. N. Phan‡
Georgia Institute of Technology, Atlanta, Georgia 30332

DOI: 10.2514/1.J051885

The linear dynamic elasticity problem formulation and solution for a generally asymmetric sandwich beam/wide plate consisting of orthotropic core and face sheets subjected to blast loading is presented. The Laplace transform is used to obtain ordinary differential equations in the complex Laplace space (the variable being the through-thickness coordinate), which are subsequently solved in closed form for a simply supported beam. The time response is then obtained by a numerical inverse Laplace transform by using the Euler method. The results for realistic material and blast cases for the transient displacements and face sheet/core interfacial transverse normal and shear stresses are presented. A comparison of the elasticity results is also made with first-order shear and high-order sandwich panel theories. This solution can be used as a benchmark in assessing the accuracy of advanced sandwich panel theories.

Nomenclature

a	=	length of the sandwich beam
c	=	half thickness of the core (total core thickness is $2c$)
c_{ij}	=	stiffness constants of the top face, bottom face, and core, respectively
E_1	=	axial extensional (Young's) modulus
$\tilde{F}(s)$	=	Laplace transform of $F(t)$
$f_{1,2}$	=	thickness of the top face and bottom face, respectively
G_{13}^c	=	shear modulus of the core
κ	=	shear correction factor
ρ	=	mass density
t	=	time
u	=	axial displacement (along x)
w	=	transverse displacement (along z)

I. Introduction

ELASTICITY solutions are significant because they provide a benchmark for assessing the performance of the various beam, plate, or shell theories, or the various numerical methods, such as the finite element method. For static problems involving laminated composite or sandwich structures a few closed-form solutions exist, namely in [1] for isotropic plates, in [2,3] for a beam and plate configuration, respectively, both under restrictive assumptions, extended in [4,5] for general sandwich plates and beams, respectively, and for a sandwich shell configuration in [6].

Sudden dynamic loading problems are more demanding on plate or beam theories than static problems or natural vibrations. Indeed, when a plate/beam is subjected to an impulsive load reflections of waves from the top and bottom surfaces, as well as higher modes and short wavelength disturbances, are not easily accounted for by plate or beam theories. The accurate prediction of stress and strain fields in the transient phase of response is important in predicting possible structural failure. It is generally believed that if the structure survives the first few milliseconds, it has survived the blast. Thus, the elasticity solutions, being most accurate, would determine the limitations of various beam/plate theories in addressing sudden loading problems.

Received 7 February 2012; revision received 9 July 2012; accepted for publication 14 July 2012; published online 6 December 2012.

*Professor, School of Aerospace Engineering.
†Professor of Structural Engineering, Technion — Israel Institute of Technology, 32000 Haifa, Israel.
‡Graduate Research Assistant, School of Aerospace Engineering; currently Postdoctoral Fellow.

For the dynamic case, an elasticity solution for the free vibration of homogeneous and laminated plates was presented in [7]. Moreover, the elasto-dynamic approach in [8] was used to study monolithic homogeneous-wide plates under lateral impulsive loadings. However, there has not been yet a dynamic elasticity study of sandwich beam/wide plates under impulse loading, which is the objective of this work.

The formulation in this paper is based on the Laplace transform of the dynamic elasticity equations. In this way, a set of ordinary differential equations with the variable being the through-thickness coordinate is obtained in the complex Laplace space. These are solved in closed form for a simply supported beam and, subsequently, the solution is obtained in the time space by the numerical inversion of the Laplace space solutions. The latter is a critical part of this research, as there exist many approaches to the numerical inversion of Laplace transforms [9], and each method is suitable for certain physical problems.

Results are derived for realistic sandwich material systems and conditions of blast. To this extent, we had guidance from the blast experiments on sandwich composites in [10]. The elasticity results are also compared to the first-order shear and the recent extended high-order sandwich panel theory (EHSAPT), which has been proven to be very accurate for the static case [11].

II. Dynamic Elasticity Formulation

We consider a sandwich beam consisting of orthotropic face sheets of thickness f_1 and f_2 and an orthotropic core of thickness $2c$, such that the various axes of elastic symmetry are parallel to the plate axes x, y, and z (Fig. 1). The body is simply supported. Although the elasticity solution is derived for any loading, results will be presented for a sudden transverse distributed loading $q_0(x, t)$ applied on the upper surface.

Let us denote each phase by i, where $i = f_1$ for the upper face sheet, $i = c$ for the core, and $i = f_2$ for the lower face sheet. The displacements along x, y, and z are denoted by u, v, and w, respectively.

The underlying assumption of the problem (two-dimensional) is

$$v = 0; \qquad u, w = \text{fn}(x, z, t) \tag{1a}$$

Using the strain-displacement relations results in

$$\epsilon_{xx} = u_{,x}; \qquad \epsilon_{zz} = w_{,z}; \qquad \gamma_{xz} = u_{,z} + w_{,x} \tag{1b}$$

and

$$\epsilon_{yy} = \gamma_{xy} = \gamma_{yz} = 0 \tag{1c}$$

Then, for each phase, the orthotropic strain-stress relations are

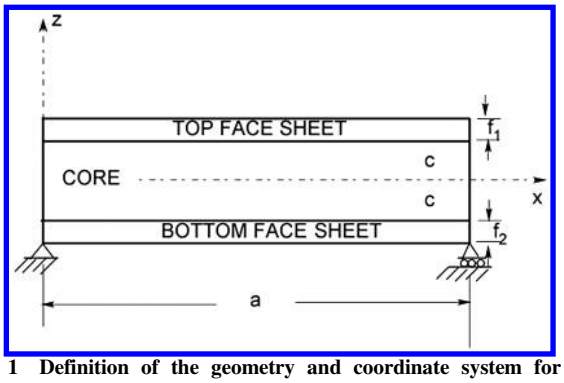

Fig. 1 Definition of the geometry and coordinate system for the sandwich beam.

$$\begin{bmatrix} \sigma_{xx}^{(i)} \\ \sigma_{yy}^{(i)} \\ \sigma_{zz}^{(i)} \\ \tau_{yz}^{(i)} \\ \tau_{xz}^{(i)} \\ \tau_{xy}^{(i)} \end{bmatrix} = \begin{bmatrix} c_{11}^i & c_{12}^i & c_{13}^i & 0 & 0 & 0 \\ c_{12}^i & c_{22}^i & c_{23}^i & 0 & 0 & 0 \\ c_{13}^i & c_{23}^i & c_{33}^i & 0 & 0 & 0 \\ 0 & 0 & 0 & c_{44}^i & 0 & 0 \\ 0 & 0 & 0 & 0 & c_{55}^i & 0 \\ 0 & 0 & 0 & 0 & 0 & c_{66}^i \end{bmatrix} \begin{bmatrix} \epsilon_{xx}^{(i)} \\ 0 \\ \epsilon_{zz}^{(i)} \\ 0 \\ \gamma_{xz}^{(i)} \\ 0 \end{bmatrix},$$

$$(i = f_1, c, f_2) \tag{2}$$

where c_{ij}^i are the stiffness constants (we have used the notation $1 \equiv x$, $2 \equiv y$, $3 \equiv z$).

Accordingly, the nonzero stresses depend only on x, z, and the time t. Thus, the dynamic equilibrium relations are

$$\sigma_{xx,x} + \tau_{xz,z} = \rho u_{,tt} \tag{3a}$$

$$\tau_{xz,x} + \sigma_{zz,z} = \rho w_{,tt} \tag{3b}$$

where ρ is the mass density.

This leads to the following governing field equations in terms of the displacements for each of the phases:

$$c_{11}^i u_{,xx} + c_{55}^i u_{,zz} + (c_{13}^i + c_{55}^i) w_{,xz} = \rho^i u_{,tt} \tag{4a}$$

$$(c_{13}^i + c_{55}^i) u_{,xz} + c_{55}^i w_{,xx} + c_{33}^i w_{,zz} = \rho^i w_{,tt} \tag{4b}$$

In the following, we shall drop the superscript i that refers to the phases (core or face sheets) with the understanding that the derived relations hold within each phase.

For a simply supported beam/wide plate an appropriate solution for the displacements would be in the form

$$u = U(z,t)\cos\, px; \qquad w = W(z,t)\sin\, px;$$
$$\text{where} \quad p = \frac{n\pi}{a} (n = 1, 2, \ldots) \tag{5}$$

Note that these displacements, in conjunction with the corresponding from Eqs. (1) and (2) stresses, would satisfy the simple support edge conditions.

Thus, Eqs. (4a) and (4b) become

$$-c_{11} p^2 U + c_{55} U_{,zz} + (c_{13} + c_{55}) p W_{,z} = \rho U_{,tt} \tag{6a}$$

$$-(c_{13} + c_{55}) p U_{,z} - c_{55} p^2 W + c_{33} W_{,zz} = \rho W_{,tt} \tag{6b}$$

We denote the Laplace transform of a function $F(t)$ by

$$\tilde{F}(s) = \int_0^\infty F(t) e^{-st}\, \mathrm{d}t \tag{7}$$

Taking the Laplace transform of Eqs. (6a) and (6b) (and assuming zero initial displacements and velocities) results in two homogeneous ordinary differential equations for the Laplace transforms of the displacements, $\tilde{U}(z)$ and $\tilde{W}(z)$:

$$-(c_{11} p^2 + \rho s^2)\tilde{U} + c_{55}\tilde{U}_{,zz} + (c_{13} + c_{55}) p \tilde{W}_{,z} = 0 \tag{8a}$$

$$-(c_{13} + c_{55}) p \tilde{U}_{,z} - (c_{55} p^2 + \rho s^2)\tilde{W} + c_{33}\tilde{W}_{,zz} = 0 \tag{8b}$$

Assuming next that

$$[\tilde{U}(z), \tilde{W}(z)] = [\tilde{U}_0, \tilde{W}_0] e^{\lambda z} \tag{9}$$

where $\tilde{U}_0$ and $\tilde{W}_0$ are constants and substituting into Eqs. (8a) and (8b) results in the following system of algebraic equations:

$$(c_{11} p^2 + \rho s^2 - c_{55}\lambda^2)\tilde{U}_0 - (c_{13} + c_{55}) p \lambda \tilde{W}_0 = 0 \tag{10a}$$

$$(c_{13} + c_{55}) p \lambda \tilde{U}_0 + (c_{55} p^2 + \rho s^2 - c_{33}\lambda^2)\tilde{W}_0 = 0 \tag{10b}$$

Nontrivial solutions of this system exist only if the determinant of the coefficients vanishes, which leads to the equation

$$A_0 \lambda^4 + A_1 \lambda^2 + A_2 = 0 \tag{11}$$

where

$$A_0 = c_{33} c_{55}, \qquad A_2 = (c_{11} p^2 + \rho s^2)(c_{55} p^2 + \rho s^2) \tag{12a}$$

$$A_1 = (c_{13} + c_{55})^2 p^2 - (c_{11} p^2 + \rho s^2) c_{33} - (c_{55} p^2 + \rho s^2) c_{55} \tag{12b}$$

With the substitution

$$\mu = \lambda^2 \tag{13a}$$

Equation (11), which defines the parameter λ, can be written in the form of a quadratic equation as

$$A_0 \mu^2 + A_1 \mu + A_2 = 0 \tag{13b}$$

Because the Laplace parameter, s, is in general complex, so are the coefficients of Eq. (13b), thus, Eq. (13b) has two complex roots:

$$\mu_{1,2} = \frac{-A_1 \pm \sqrt{A_1^2 - 4A_0 A_2}}{2A_0} \tag{13c}$$

which results in four complex roots of Eq. (11):

$$\lambda_{1,2} = \pm\sqrt{\mu_1}; \qquad \lambda_{3,4} = \pm\sqrt{\mu_2} \tag{13d}$$

Corresponding to these four roots the transformed displacement functions take the form

$$\tilde{U}(z) = \sum_{i=1,2,3,4} a_i e^{\lambda_i z}; \qquad \tilde{W}(z) = \sum_{i=1,2,3,4} b_i e^{\lambda_i z} \tag{14a}$$

where a_i and b_i are complex constants.

Of the eight constants appearing in Eq. (14) only four are independent. The four relations that exist among these constants are found by substituting the transformed displacements in Eq. (14) into the equilibrium Eqs. (8a) and (8b). In this way, we obtain the following relations for the coefficients in the transformed displacement expression for $\tilde{W}(z)$, Eq. (14), in terms of the coefficients in the expression for $\tilde{U}(z)$:

$$b_i = \frac{[(c_{11}p^2 + \rho s^2) - c_{55}\lambda_i^2]}{(c_{13} + c_{55})p\lambda_i} a_i \tag{14b}$$

Hence, if we consider as independent the four constants a_i, $i = 1, 4$, we can write the transformed displacement $\tilde{u}(x, z)$ in the form

$$\tilde{u} = \sum_{i=1,2,3,4} d_{ui} a_i \cos px \tag{15a}$$

with the z-dependent coefficients defined as

$$d_{ui} = e^{\lambda_i z} \tag{15b}$$

The transformed displacement $\tilde{w}(x, z)$ is in the form

$$\tilde{w} = \sum_{i=1,2,3,4} d_{wi} a_i \sin px \tag{15c}$$

where the z-dependent coefficients are defined:

$$d_{wi} = \frac{(c_{11}p^2 + \rho s^2) - c_{55}\lambda_i^2}{(c_{13} + c_{55})p\lambda_i} e^{\lambda_i z} \tag{15d}$$

The corresponding stresses are derived by substituting the above displacement expressions into Eqs. (1) and (2). We present the explicit expressions for the stresses in the following equations.

The transformed transverse normal stress $\tilde{\sigma}_{zz}(x, z)$ is in the form

$$\tilde{\sigma}_{zz} = \sum_{i=1,2,3,4} b_{zzi} a_i \sin px \tag{16a}$$

with the z-dependent coefficients defined as

$$b_{zzi} = \left\{ -c_{13}p + c_{33} \frac{[(c_{11}p^2 + \rho s^2) - c_{55}\lambda_i^2]}{(c_{13} + c_{55})p} \right\} e^{\lambda_i z} \tag{16b}$$

The transformed shear stress $\tilde{\tau}_{xz}(x, z)$ is in the form

$$\tilde{\tau}_{xz} = \sum_{i=1,2,3,4} b_{xzi} a_i \cos px \tag{17a}$$

with the z-dependent coefficients defined as

$$b_{xzi} = c_{55} \left\{ \lambda_i + \frac{[(c_{11}p^2 + \rho s^2) - c_{55}\lambda_i^2]}{(c_{13} + c_{55})\lambda_i} \right\} e^{\lambda_i z} \tag{17b}$$

Finally, the transformed axial stress $\tilde{\sigma}_{xx}$ is in the form

$$\tilde{\sigma}_{xx} = \sum_{i=1,2,3,4} b_{xxi} a_i \sin px \tag{18a}$$

with the z-dependent coefficients defined as

$$b_{xxi} = \left\{ -c_{11}p + c_{13} \frac{[(c_{11}p^2 + \rho s^2) - c_{55}\lambda_i^2]}{(c_{13} + c_{55})p} \right\} e^{\lambda_i z} \tag{18b}$$

From this analysis, we can see that within each phase (i), where $i = f_1, c, f_2$, there are four constants: $a_j^{(i)}$, $j = 1, \ldots 4$. Therefore, for the three phases, this gives a total of 12 constants to be determined.

There are two traction conditions at each of the two core/face sheet interfaces giving a total of four conditions. In a similar fashion, there are two displacement continuity conditions at each of the two core/face sheet interfaces giving another four conditions. Finally, there are 2 traction boundary conditions on each of the 2-plate bounding surfaces, giving another 4 conditions for a total of 12 equations.

Thus, the solution for the transformed displacements, stresses, and strains follows accordingly as outlined above in terms of the constants $a_j^{(f2)}$, $a_j^{(c)}$, and $a_j^{(f1)}$, $j = 1, 4$. These 12 constants are determined as follows:

There are two traction conditions at the lower face sheet/core interface, $z = -c$:

1) The $\tilde{\sigma}_{zz}^{(c)} = \tilde{\sigma}_{zz}^{(f2)}$ at $z = -c$, which gives

$$\sum_{j=1,2,3,4} b_{zzj}^{(c)} \Big|_{z=-c} a_j^{(c)} = \sum_{j=1,2,3,4} b_{zzj}^{(f2)} \Big|_{z=-c} a_j^{(f2)} \tag{19a}$$

and

2) the $\tilde{\tau}_{xz}^{(c)} = \tilde{\tau}_{xz}^{(f2)}$ at $z = -c$, which gives

$$\sum_{j=1,2,3,4} b_{xzj}^{(c)} \Big|_{z=-c} a_j^{(c)} = \sum_{j=1,2,3,4} b_{xzj}^{(f2)} \Big|_{z=-c} a_j^{(f2)} \tag{19b}$$

There are also two displacement continuity conditions at the lower core/face sheet interfaces:

3) The $\tilde{U}^{(c)} = \tilde{U}^{(f2)}$ at $z = -c$, which results in

$$\sum_{j=1,2,3,4} d_{uj}^{(c)} \Big|_{z=-c} a_j^{(c)} = \sum_{j=1,2,3,4} d_{uj}^{(f2)} \Big|_{z=-c} a_j^{(f2)} \tag{19c}$$

and finally

4) the $\tilde{W}^{(c)} = \tilde{W}^{(f2)}$ at $z = -c$, which gives

$$\sum_{j=1,2,3,4} d_{wj}^{(c)} \Big|_{z=-c} a_j^{(c)} = \sum_{j=1,2,3,4} d_{wj}^{(f2)} \Big|_{z=-c} a_j^{(f2)} \tag{19d}$$

Next, there are two traction conditions at the upper face sheet/core interface, $z = +c$:

5) $\tilde{\sigma}_{zz}^{(f1)} = \tilde{\sigma}_{zz}^{(c)}$ at $z = +c$, which gives

$$\sum_{j=1,2,3,4} b_{zzj}^{(c)} \Big|_{z=+c} a_j^{(c)} = \sum_{j=1,2,3,4} b_{zzj}^{(f1)} \Big|_{z=+c} a_j^{(f1)} \tag{20a}$$

and

6) $\tilde{\tau}_{xz}^{(f1)} = \tilde{\tau}_{xz}^{(c)}$ at $z = +c$, which gives

$$\sum_{j=1,2,3,4} b_{xzj}^{(c)} \Big|_{z=+c} a_j^{(c)} = \sum_{j=1,2,3,4} b_{xzj}^{(f1)} \Big|_{z=+c} a_j^{(f1)} \tag{20b}$$

The corresponding displacement continuity conditions at the upper face sheet/core interface, $z = +c$ are

7) $\tilde{U}^{(f1)} = \tilde{U}^{(c)}$ at $z = +c$, which gives

$$\sum_{j=1,2,3,4} d_{uj}^{(c)} \Big|_{z=+c} a_j^{(c)} = \sum_{j=1,2,3,4} d_{uj}^{(f1)} \Big|_{z=+c} a_j^{(f1)} \tag{20c}$$

and

8) $\tilde{W}^{(f1)} = \tilde{W}^{(c)}$ at $z = +c$, which gives

$$\sum_{j=1,2,3,4} d_{wj}^{(c)} \Big|_{z=+c} a_j^{(c)} = \sum_{j=1,2,3,4} d_{wj}^{(f1)} \Big|_{z=+c} a_j^{(f1)} \tag{20d}$$

Finally, two traction conditions exist on each of the two bounding surfaces. The traction free conditions at the lower bounding surface, $z = -(c + f_2)$, can be written as follows:

9) $\tilde{\sigma}_{zz}|_{z=-(c+f2)} = 0$, which gives

$$\sum_{j=1,2,3,4} b_{zzj}^{(f2)} \Big|_{z=-(c+f_2)} a_j^{(f2)} = 0 \tag{21a}$$

and

(10) $\tilde{\tau}_{xz}|_{z=-(c+f2)} = 0$, which gives

$$\sum_{j=1,2,3,4} b_{xzj}^{(f2)} \Big|_{z=-(c+f_2)} a_j^{(f2)} = 0 \tag{21b}$$

We assume that a transverse distributed loading $q_0(x,t)$ per unit width is applied at the top face sheet. If the form of the distributed load is

$$q_0(x,t) = Q_0(t)\sin\frac{n\pi x}{a} = Q_0(t)\sin\ px \tag{22}$$

and the Laplace transform of $Q_0(t)$ is $\tilde{Q}_0(s)$, then at the upper bounding surface where the transverse load $q_0(x,t)$ is applied, we have the condition

11) $\tilde{\sigma}_{zz}|_{z=(c+f1)} = \tilde{Q}_0(s)\sin\ px$ which gives

$$\sum_{j=1,2,3,4} b_{zzj}^{(f1)}\Big|_{z=(c+f1)} a_j^{(f1)} = \tilde{Q}_0(s) \tag{23a}$$

For example, for an exponential decay loading $Q_0(t) = A_0 e^{-t/c}$ we would have $\tilde{Q}_0(s) = A_0 c/(1+sc)$.

For a pulse loading of amplitude A_0 and of infinite duration, $Q_0(t) = A_0 H(t)$, where H is the Heaviside unit function, we would have $\tilde{Q}_0(s) = A_0/s$ and for a pulse loading of amplitude A_0 and of finite duration t_0, we would have $\tilde{Q}_0(s) = A_0(1-e^{-t_0 s})/s$.

Moreover, we have the second traction condition at the bounding surface of the top face sheet

12) $\tilde{\tau}_{xz}|_{z=(c+f1)} = 0$, which gives

$$\sum_{j=1,2,3,4} b_{xzj}^{(f1)}\Big|_{z=(c+f1)} a_j^{(f1)} = 0 \tag{23b}$$

Therefore, we have a system of 12 linear algebraic equations in the 12 (in general complex) unknowns, $a_j^{(f2)}$, $a_j^{(c)}$, and $a_j^{(f1)}$, $j = 1, 4$. Solving for these determines in closed form the Laplace transforms of the displacement and stress fields.

The next step is the inversion back to the time space, which is done numerically. This a critical part of this research, as there exist many approaches to the numerical inversion of Laplace transforms [9] and each method is suitable for certain physical problems, for example, different methods would be needed for heat transfer problems as opposed to structural vibration problems. The Euler method, as described in [12], was found to provide excellent accuracy by comparing its application to the closed-form classical beam theory vibration equations of a simple homogeneous beam of the same overall stiffness as our sandwich beam. The numerical inversion based on the Euler method produced results in the time space that were exactly the theoretical results up to a time of about 10 ms.

The Euler method, so named because it employs Euler summation, is based on the Bromwich contour inversion integral, which can be expressed as the integral of a real-valued function of a real variable by choosing a specific contour [12]. The integral is calculated by the use of the Fourier-series method (the Poisson summation formula) and the Euler summation to accelerate convergence. In addition to confirming the numerical inversion by comparing to the closed-form simple vibration equation, the accuracy was further confirmed in the time scale of interest by comparing with the results from the Post–Widder method, again described in [12]. It should be noticed that both the Euler and the Post–Widder methods are variants of the Fourier-series method, but they are dramatically different so that they can be expected to serve as useful checks on each other.

A. First-Order Shear Sandwich Beam Theory

For the first-order shear deformation (FOSD) model, if we let ψ be the shear deformation then the governing dynamic equations with shear effects can be written as

$$D_{11}\psi_{,xx}(x,t) - \kappa D_{55}[\psi(x,t) + w_{,x}(x,t)] = (\rho I)_{\text{eq}}\frac{\partial^2\psi(x,t)}{\partial t^2} \tag{24a}$$

$$\kappa D_{55}[\psi_{,x}(x,t) + w_{,xx}(x,t)] + q(x,t) = (\rho h)_{\text{eq}}\frac{\partial^2 w(x,t)}{\partial t^2} \tag{24b}$$

Although the shear correction factor in homogeneous sections is taken typically as $\kappa = 5/6$ in a sandwich section, the shear stress distribution in the core is largely uniform and, therefore, we set $\kappa = 1$ as the shear correction factor. Moreover, in the general asymmetric case, the neutral axis of the sandwich section is defined at a distance e from the x axis (Fig. 1):

$$e(E_1^t f_1 + E_1^b f_2) = E_1^t f_t\left(\frac{f_1}{2}+c\right) - E_1^b f_2\left(\frac{f_2}{2}+c\right) \tag{25a}$$

Therefore, the bending stiffness per unit width, D_{11}, is

$$D_{11} = E_1^t\frac{f_1^3}{12} + E_1^t f_1\left(\frac{f_1}{2}+c-e\right)^2 + E_1^b\frac{f_2^3}{12} + E_1^b f_2\left(\frac{f_2}{2}+c+e\right)^2 \tag{25b}$$

The core is assumed to be the only contributor to the sandwich shear modulus, thus

$$D_{55} = G_{13}^c(2c) \tag{26}$$

Furthermore, $(\rho h)_{\text{eq}}$ is defined from the densities and thicknesses of the faces and the core as

$$(\rho h)_{\text{eq}} = \rho_t f_1 + \rho_c(2c) + \rho_b f_2 \tag{27}$$

and $(\rho I)_{\text{eq}}$ is defined from the densities and the moments of inertia of the faces and the core with respect to the neutral axis for the sandwich section as

$$(\rho I)_{\text{eq}} = \rho_t\left[\frac{f_1^3}{12} + f_1\left(\frac{f_1}{2}+c-e\right)^2\right] + \rho_c\left[\frac{(2c)^3}{12} + (2c)e^2\right] + \rho_b\left[\frac{f_2^3}{12} + f_2\left(\frac{f_2}{2}+c+e\right)^2\right] \tag{28}$$

Setting

$$w(x) = W(t)\sin\ px; \qquad \psi(x) = \Psi(t)\cos\ px; \qquad p = \frac{n\pi}{a} \tag{29}$$

with the load in the same manner as Eq. (22), and substituting in Eqs. (24a) and (24b) leads to

$$-D_{11}p^2\Psi(t) - \kappa D_{55}[\Psi(t) + pW(t)] = (\rho I)_{\text{eq}}\frac{\mathrm{d}^2\Psi(t)}{\mathrm{d}t^2} \tag{30a}$$

$$-\kappa D_{55}p[\Psi(t) + pW(t)] + Q(t) = (\rho h)_{\text{eq}}\frac{\mathrm{d}^2 W(t)}{\mathrm{d}t^2} \tag{30b}$$

Taking the Laplace transforms gives

$$-D_{11}p^2\tilde{\Psi} - \kappa D_{55}(\tilde{\Psi} + p\tilde{W}) = (\rho I)_{\text{eq}}s^2\tilde{\Psi} \tag{31a}$$

$$-\kappa D_{55}(p\tilde{\Psi} + p^2\tilde{W}) + \tilde{q} = (\rho h)_{\text{eq}}\tilde{s}^2 W(t) \tag{31b}$$

These two algebraic equations give

$$\tilde{W} = \tilde{Q}_0\frac{s^2(\rho I)_{\text{eq}} + p^2 D_{11} + kD_{55}}{[s^2(\rho h)_{\text{eq}} + p^2 kD_{55}][s^2(\rho I)_{\text{eq}} + p^2 D_{11} + kD_{55}] - p^2 k^2 D_{55}^2} \tag{32}$$

The inversion of the above equation is implemented in the same way as for the elasticity, i.e., the Euler method, as described in [12].

III. Results and Discussion

We produce results for a sandwich system material and loading as in the experiments in [13]. The faces are made out of glass vinyl ester with $E_1^f = E_2^f = E_3^f = 13.6$ GPa, $\nu_{12}^f = \nu_{13}^f = 0.25$ and $\nu_{32}^f = 0.35$, and the density $\rho_f = 1800$ kg/m^3. The core is made out of Corecell foam with $E_1^c = E_2^c = E_3^c = 0.032$ GPa, $\nu_{12}^c = \nu_{13}^c = 0.25$ and $\nu_{32}^c = 0.35$, and the density $\rho_c = 58.5$ kg/m^3. The sandwich is symmetric with the face thickness $f = 5$ mm, the core thickness $2c = 38$ mm, and the length $a = 152.4$ mm. The width is $b = 102$ mm.

For the sake of simplicity, we assume a single half-wave sinusoidal loading, i.e., in Eq. (22), $n = 1$. Note that a general loading can be expanded in a series of terms of the type (22) anyway.

The time dependence of the loading is constructed from the shock wave history reported in [13] and is expressed in the form of an exponentially decaying blast:

$$Q_0(t) = -0.51e^{-1.25t}\ \text{MN/mm(t in sec)}$$

Thus, the Laplace transform of the load is

$$\tilde{Q}_0(s) = -0.51/(s + 1.25)$$

For each phase, the stiffness constants c_{ij}, that enter into the solution are found from

$$c_{11} = E_1\frac{(1-\nu_{23}\nu_{32})}{C_0}; \qquad c_{13} = E_3\frac{(\nu_{13}+\nu_{12}\nu_{23})}{C_0} \tag{33a}$$

$$c_{33} = E_3\frac{(1-\nu_{12}\nu_{21})}{C_0}, \qquad c_{55} = G_{31} \tag{33b}$$

where

$$C_0 = 1 - (\nu_{12}\nu_{21} + \nu_{23}\nu_{32} + \nu_{13}\nu_{31}) - (\nu_{12}\nu_{23}\nu_{31} + \nu_{21}\nu_{13}\nu_{32}) \tag{33c}$$

Plotted in Fig. 2a is the transverse displacement, w, of the midtop face, midcore, and midbottom face, and at midspan, $x = a/2$, as a function of time during the first 2 ms. It can be seen that the bottom face is lagging the top face, whereas the core is also following a different path. The displacements are of the same scale as the measured ones in [10]. At about 0.6–0.7 ms, which is the peak of the top face displacement, it can be seen that the top face is displacing by 3–4 mm more than the bottom face, thus, the core is substantially compressed. This time scale of noticeable core reduction in thickness agrees with the experimental observations in [13]. The differences between faces and core become small beyond 1 ms, and eventually both faces and the core displace in tandem (beyond around 1.6 ms).

The FOSD displacements are shown in Fig. 2b, and it can be seen in the following:

1) The FOSD theory cannot capture the divergences and lag behavior between faces and core.

2) The FOSD theory significantly overestimates the dynamic displacements.

On this observation, it should be noted that the results of the FOSD theory depend heavily on the shear rigidity of the panel. As shown in [11], which was for the static case, if the FOSD theory is formulated with the panel shear rigidity based exclusively on the core, then the FOSD theory transverse displacement is larger than that from elasticity. If, however, the FOSD theory is formulated with the panel shear rigidity including the face sheets, then the FOSD theory transverse displacement is smaller than that from elasticity. In the present paper, which is for the dynamic case, the FOSD theory was formulated with the panel shear rigidity based exclusively on the core, Eq. (26), thus, the results in Fig. 2b showing the FOSD theory displacements larger than those from elasticity are not surprising.

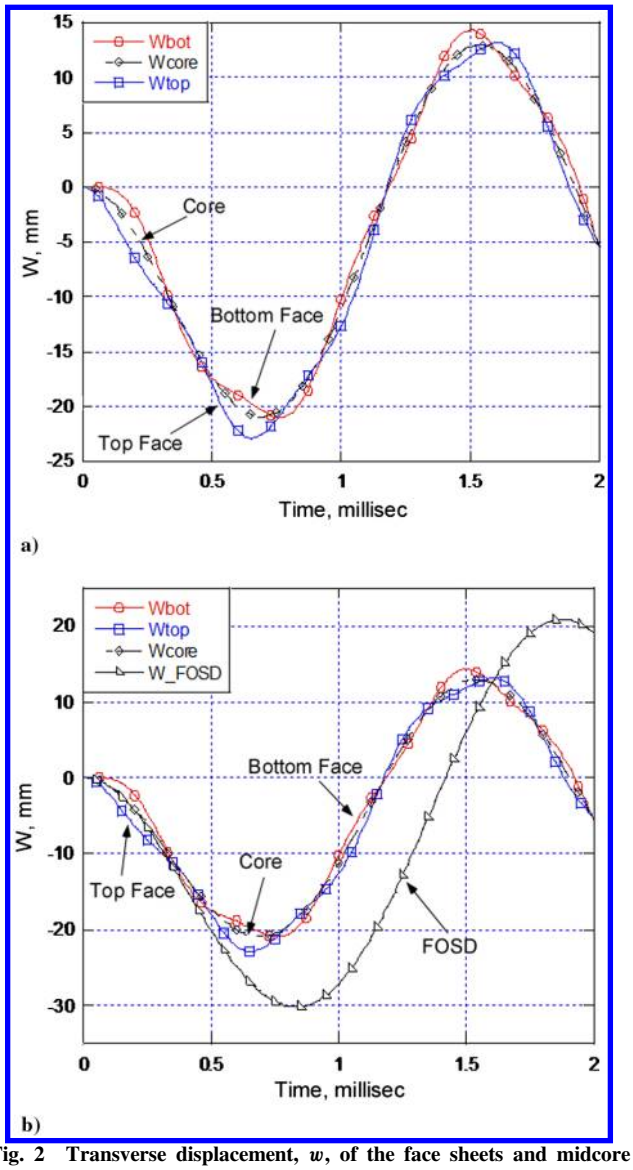

Fig. 2 Transverse displacement, w, of the face sheets and midcore during the first 2 ms: a) dynamic elasticity detail; b) FOSD vs elasticity.

Figure 3 shows the axial displacement, u, at the middle of the faces and the core at $x = 0$, and the important observation is the high frequency and relatively large amplitude cyclic behavior in the core unlike the faces.

The interfacial shear stress, τ_{xz}, during the first 2 ms at $x = 0$ is shown in Fig. 4. Initially, the τ_{xz} is quite different between the two interfaces, and at 0.5–0.7 ms the bottom face sheet interface shows quite noticeably higher shear stress than the top one. However, after about 1.6 ms the two interfaces exhibit the same shear stress. In this time interval, the shear stress switches the sign and follows the cyclic behavior of the transverse displacement. The magnitude of the shear stress at the interfaces is considerable and, given the fact that inside the core there would be shear stresses of similar magnitude, it can explain the core cracking initiating after about 0.5 ms, which was observed in the experiments [13].

On the contrary, the interfacial normal stress, σ_{zz}, follows the cyclic behavior of the core and is shown in Fig. 5 at midspan, $x = a/2$. It can be seen that the bottom face/core interface goes into appreciable tension, whereas the top face/core interface is always in compression during the first 1 ms but can go into tension afterwards. This, together with the high values of interfacial shear stress, can help explain the skin delamination observed in the experiments after 1 ms [13].

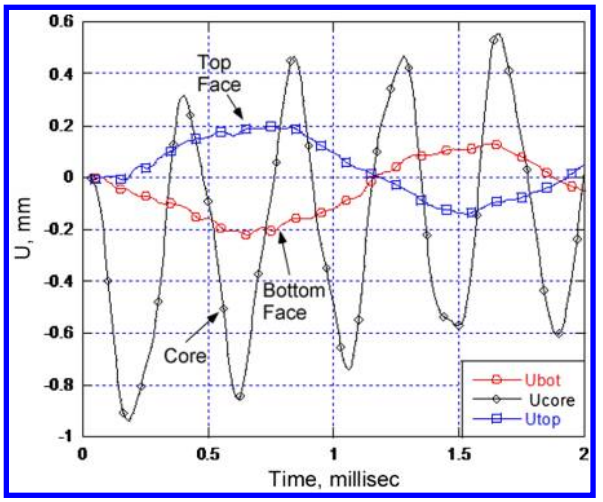

Fig. 3 Axial displacement, u, at the middle of the faces and the core during the first 2 ms.

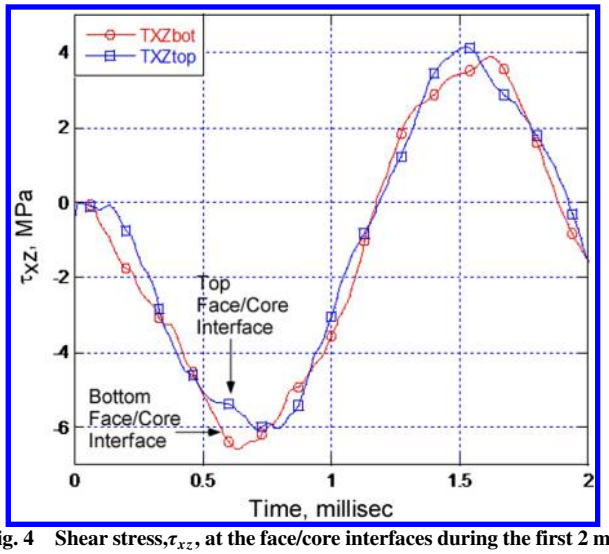

Fig. 4 Shear stress, τ_{xz}, at the face/core interfaces during the first 2 ms.

The dynamic elasticity results are next compared with results from the recent dynamic EHSAPT [14]. Figure 6 shows a comparison of the transverse displacement at the top face/core interface location. The dynamic elasticity shows very good agreement with the dynamic EHSAPT.

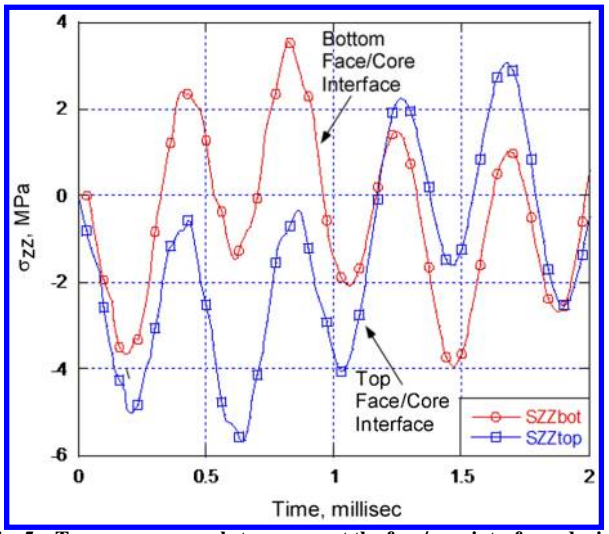

Fig. 5 Transverse normal stress, σ_{zz}, at the face/core interfaces during the initial phase of blast.

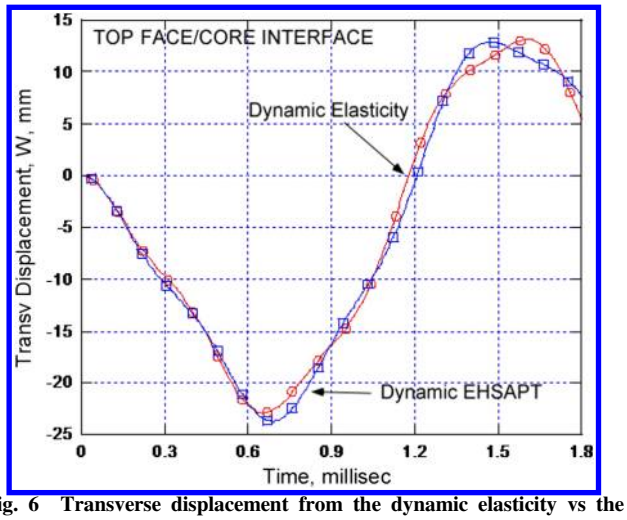

Fig. 6 Transverse displacement from the dynamic elasticity vs the EHSAPT at the top face/core interface.

IV. Conclusions

A dynamic elasticity solution for the transient response of a sandwich beam/wide plate consisting of orthotropic core and face sheets subjected to blast loading at the top face was presented. The problem was formulated in terms of Laplace transforms. The results for a realistic material and blast case reveal that during the transient phase the face and core displacements are different with the bottom face exhibiting appreciable lagging as compared to the top face, whereas the core is also following a different path. These divergences and lag behavior between faces and the core cannot be captured by the first-order shear deformation theory, but they are very well captured by the extended high-order sandwich panel theory (EHSAPT). Futhermore, the interfacial normal stress exhibits a cyclic behavior during the transient phase with the bottom face/core interface going into appreciable tension, whereas the top face/core interface is always in compression. The interfacial shear stress is also quite different between the two interfaces, and the bottom face/core interface shows noticeably higher shear stress than the top one during the initial phase. This elasticity solution can be used as a benchmark in assessing the accuracy of the various sandwich panel theories.

Acknowledgments

The financial support of the Office of Naval Research, grant no. N00014-11-1-0597, and the interest and encouragement of the grant monitor, Y. D. S. Rajapakse, are both gratefully acknowledged.

References

[1] Vlasov, B. F., "On One Case of Bending of Rectangular Thick Plates," Vestnik Moskovskogo Universiteta, Serieii'a Matematiki, mekhaniki, astronomii, fiziki, khimii, No. 2, 1957, p. 2534.

[2] Pagano, N. J., "Exact Solutions for Composite Laminates in Cylindrical Bending," *Journal of Composite Materials*, Vol. 3, July 1969, pp. 398–411. doi:10.1177/002/99836900300304

[3] Pagano, N. J., "Exact Solutions for Rectangular Bidirectional Composites and Sandwich Plates," *Journal of Composite Materials*, Vol. 4, Jan. 1970, pp. 20–34.

[4] Kardomateas, G. A., "Three Dimensional Elasticity Solution for Sandwich Plates with Orthotropic Phases: the Positive Discriminant Case," *Journal of Applied Mechanics*, Vol. 76, 2009, p. 014505. doi:10.1115/1.2966174

[5] Kardomateas, G. A., and Phan, C. N., "Three Dimensional Elasticity Solution for Sandwich Beams/Wide Plates with Orthotropic Phases: the Negative Discriminant Case," *Journal of Sandwich Structures and Materials*, Vol. 13, No. 6, Nov. 2011, pp. 641–661. doi:10.1177/1099636211419127

[6] Kardomateas, G. A., "Elasticity Solutions for a Sandwich Orthotropic Cylindrical Shell Under External Pressure, Internal Pressure and Axial Force," *AIAA Journal*, Vol. 39, No. 4, 2001, pp. 713–719. doi:10.2514/2.1366

[7] Srinivas, S., Joga Rao, C. V., and Rao, A. K., "An Exact Analysis for Vibration of Simply-Supported Homogeneous and Laminated Thick Rectangular Plates," *Journal of Sound and Vibration*, Vol. 12, No. 2, 1970, pp. 187–199. doi:10.1016/0022-460X(70)90089-1

[8] Sun, C. T., and Lai, R. Y. S., "Exact and Approximate Analyses of Transient Wave Propagation in an Anisotropic Plate," *AIAA Journal*, Vol. 12, No. 10, 1974, pp. 1415–1417. doi:10.2514/3.49500

[9] Cohen, A. M., *Numerical Methods for Laplace Transform Inversion*, Springer–Verlag, New York, NY, 2007.

[10] Wang, E., and Shukla, A., "Blast Performance of Sandwich Composites with In-Plane Compressive Loading," *Experimental Mechanics*, Vol. 52, No. 1, Jan. 2012, pp. 49–58. doi:10.1007/S11340-011-9500-5

[11] Phan, C. N., Frostig, Y., and Kardomateas, G. A., "Analysis of Sandwich Panels with a Compliant Core and with In-Plane Rigidity-Extended High-Order Sandwich Panel Theory Versus Elasticity," *Journal of Applied Mechanics*, Vol. 79, 2012, p. 041001. doi:10.1115/1.4005550

[12] Abate, J., and Whitt, W., "Numerical Inversion of Laplace Transforms of Probability Distributions," *ORSA Journal on Computing*, Vol. 7, No. 1, 1995, pp. 38–43. doi:10.1287/ijoc.7.1.36

[13] Gardner, N., Wang, E., Kumar, P., and Shukla, A., "Blast Mitigation in a Sandwich Composite Using Graded Core and Polyurea Interlayer," *Experimental Mechanics*, Vol. 52, No. 2, Feb. 2012, pp. 119–133. doi:10.1007/S11340-011-9517-9.

[14] Phan, C. N., Frostig, Y., and Kardomateas, G. A., "The Dynamic Extended High-Order Sandwich Panel Theory and Application to Blast Response of a Sandwich Panel," *Journal of Applied Mechanics* (in press).

S. Pellegrino
Associate Editor